Internal structure of Skyrme black hole

Takashi Tamaki * and Kei-ichi Maeda†

Department of Physics, Waseda University, Ohkubo, Shinjuku, Tokyo 169-8555, Japan

Takashi Torii ‡

Research Center for the Early Universe, University of Tokyo, Hongo, Bunkyo, Tokyo 113-0033, Japan

and

Advanced Research Institute for Science and Engineering, Waseda University, Ohkubo, Shinjuku, Tokyo 169-8555, Japan

(February 7, 2008)

We consider the internal structure of the Skyrme black hole under a static and spherically symmetric ansatz. We concentrate on solutions with the node number one and with the "winding" number zero, where there exist two solutions for each horizon radius; one solution is stable and the other is unstable against linear perturbation. We find that a generic solution exhibits an oscillating behavior near the sigularity, as similar to a solution in the Einstein-Yang-Mills (EYM) system, independently to stability of the solution. Comparing it with that in the EYM system, this oscillation becomes mild because of the mass term of the Skyrme field. We also find Schwarzschild-like exceptional solutions where no oscillating behavior is seen. Contrary to the EYM system where there is one such solution branch if the node number is fixed, there are two branches corresponding to the stable and the unstable ones.

04.40.-b, 04.70.-s, 95.30.Tg. 97.60.Lf.

I. INTRODUCTION

After the discovery of the Bartnik-Mckinnon solution in the SU(2) Einstein-Yang-Mills (EYM) system [1], many particle-like and black hole solutions were found and argued in extended systems such as the EYM-Higgs (EYMH) system and the EYM-dilaton (EYMD) system [2]. They are important as counterexamples of the black hole no hair conjecture [3]. Moreover, recent investigations show that the internal structure of a black hole in the SU(2) EYM system exhibits interesting behaviors which are not found in the Kerr-Newman black holes [4,5]. A generic solution in the EYM system exhibits an infinitely oscillating behavior near the sigularity, which can be understood by reducing the equations to a simplified dynamical system. Though this oscillation becomes more violent towards the singularity, it is not chaotic. This result is extended to other systems such as the EYMH system [5,6] and the EYMD system [7]. In these cases, a scalar field plays a crucial role in preventing such behaviors.

At present, the internal structure of the Einstein-Skyrme (ES) system has not been analyzed by previous researches [8–10]. This system, however, may provide us an interesting example, since the mass term of the Skyrme field can give nontrivial effects when we reduce this system to the simplified dynamical system [11]. If we see the ES system as an effective theory of the EYMH system, it is plausible that the oscillating behavior may be stopped in spite of the absence of the scalar field. Moreover, we are interested in its relation to the stability of black holes. As a common feature to the EYMH system, there are two black hole solutions in the ES system if we fix the horizon radius, the node number and the "winding" number [10,12]. This result was also extended to Brans-Dicke theory [13]. One of the solutions is similar to the Schwarzschild black hole and stable, and the other to the black hole in the EYM system and unstable. We want to know how the difference of these solutions are reflected in their internal structures. After describing our model, we investigate these features and compare them with those in the EYM system. Throughout this paper, we use the units $c = \hbar = 1$.

II. MODEL AND BASIC EQUATIONS

We start with the following action.

$$S = \int d^4x \sqrt{-g} \left[\frac{1}{2\kappa^2} R + L_m \right] , \qquad (1)$$

where $\kappa^2 := 8\pi G$ with G being Newton's gravitational constant. L_m is the Lagrangian of the matter field. We choose the Skyrme field L_m, which is $SU(2) \times SU(2)$ invariant and is given as [14]

$$L_m = -\frac{1}{32g_s^2} \mathrm{Tr} \boldsymbol{F}^2 - \frac{f_s^2}{4} \mathrm{Tr} \boldsymbol{A}^2 , \qquad (2)$$

where f_s and g_s are coupling constants. In our convention, g_s is related to the coupling constant of the Yang-Mills field g_c as $g_s = \sqrt{4\pi} g_c$. The "mass" parameter of the Skyrme field is defined by $\mu := f_s g_s$. $\boldsymbol{F}$ and $\boldsymbol{A}$ are the field strength and its potential, respectively. They are described by the $SU(2)$-valued function $\boldsymbol{U}$ as

*electronic mail:tamaki@gravity.phys.waseda.ac.jp

†electronic mail:maeda@gravity.phys.waseda.ac.jp

‡electronic mail:torii@resceu.s.u-tokyo.ac.jp

$$\boldsymbol{F} = \boldsymbol{A} \wedge \boldsymbol{A}, \quad \boldsymbol{A} = \boldsymbol{U}^{\dagger} \nabla \boldsymbol{U} . \tag{3}$$

In this paper, we consider the static and spherically symmetric metric,

$$ds^2 = -C(r)e^{2\delta(r)}dt^2 + C(r)^{-1}dr^2 + r^2 d\Omega_2^{\ 2} , \tag{4}$$

where $C(r) =: 1 - 2Gm(r)/r$. In this case, we can set $\boldsymbol{U}$,

$$\boldsymbol{U}(\chi) = \cos \chi(r) + i \sin \chi(r) \boldsymbol{\sigma}_i \hat{r}^i , \tag{5}$$

where $\boldsymbol{\sigma}_i$ and $\hat{r}^i$ are the Pauli spin matrices and a radial normal, respectively. The boundary condition for a black hole solution at spatial infinity is,

$$\lim_{r \to \infty} m = M < \infty, \quad \lim_{r \to \infty} \delta = 0 . \tag{6}$$

For the existence of a regular event horizon, r_h, we have

$$m_h := m(r_h) = \frac{r_h}{2G}, \quad \delta_h := \delta(r_h) < \infty . \tag{7}$$

We also require that no singularity exists outside the horizon, i.e.,

$$m(r) < \frac{r}{2G} \qquad \text{for} \quad r > r_h. \tag{8}$$

The boundary condition of a Skyrme field for the total field energy to be finite is written generically as

$$\lim_{r \to \infty} \chi = 0 . \tag{9}$$

For our numerical calculation, we introduce the following dimensionless variables:

$$\bar{r} = r/r_h, \ \bar{m} = Gm/r_h. \tag{10}$$

We also define dimensionless parameters as

$$\bar{f}_s := f_s/m_p, \ \lambda_h = r_h/(l_p/g_c) . \tag{11}$$

$l_p := G^{1/2}$ and $m_p := G^{-1/2}$ are the Planck length and mass defined by Newton's gravitational constant, respectively. The basic equations are now

$$\frac{d\bar{m}}{d\bar{r}} = \frac{1}{\lambda_h^2} \left[BC \left(\frac{d\chi}{d\bar{r}} \right)^2 + \frac{A \sin^2 \chi}{2\bar{r}^2} \right] , \tag{12}$$

$$\frac{d\delta}{d\bar{r}} = -\frac{2B}{\lambda_h^2 \bar{r}} \left(\frac{d\chi}{d\bar{r}} \right)^2 , \tag{13}$$

$$\frac{d^2\chi}{d\bar{r}^2} = -\frac{1}{2B} \left(8\pi \lambda_h^2 \bar{f}_s^2 \bar{r} + \frac{d\chi}{d\bar{r}} \sin 2\chi \right) \frac{d\chi}{d\bar{r}}$$
$$+ \frac{1}{C} \left[\frac{\sin 2\chi}{2B} \left(4\pi \lambda_h^2 \bar{f}_s^2 + \frac{\sin^2 \chi}{\bar{r}^2} \right) \right.$$
$$\left. + \frac{d\chi}{d\bar{r}} \left(\frac{A \sin^2 \chi}{\lambda_h^2 \bar{r}^3} - \frac{2\bar{m}}{\bar{r}^2} \right) \right] , \tag{14}$$

where we use abbreviations as

$$A := 8\pi \lambda_h^2 \bar{f}_s^2 \bar{r}^2 + \sin^2 \chi , \tag{15}$$
$$B := 2\pi \lambda_h^2 \bar{f}_s^2 \bar{r}^2 + \sin^2 \chi . \tag{16}$$

As we can see above, the metric function δ is decoupled in the equations and calculated by just integrating Eq. (13) after we obtain the solution $\chi(r)$ and $m(r)$. The square bracket in Eq. (14) must vanish at $r = r_h$ for the horizon to be regular. Hence

$$\left. \frac{d\chi}{d\bar{r}} \right|_{\bar{r}=1} = -\frac{\lambda_h^2 \sin 2\chi_h (4\pi \bar{f}_s^2 \lambda_h^2 + \sin^2 \chi_h)}{2B_h (A_h \sin^2 \chi_h - \lambda_h^2)} , \tag{17}$$

where $\chi_h := \chi(r_h)$ is a shooting parameter and should be determined iteratively so that the boundary conditions (6) and (9) are satisfied.

III. RESULTS

First, we briefly review main properties of the Skyrme black holes analyzed in Ref. [12]. We show the relation between the gravitational mass M and the horizon radius r_h in Fig. 1. As the colored black hole, i.e., the black hole solution in the EYM system, these solutions are also characterized by the node number. We choose solutions of node number one. For Skyrme black holes [8,9], the solutions are also characterized by the "winding" number defined by [15]

$$W_n := \frac{1}{\pi} |\chi_h - \chi(\infty) - \sin(\chi_h)| . \tag{18}$$

We consider solutions with the "winding" number close to one (it is ~ 1 near the zero horizon limit and ~ 0.75 near the cusp in Fig. 1.) with $\bar{f}_s = 0.02$ and 0.03 in Fig. 1. We also show the colored and Schwarzschild black hole cases, which correspond to $\bar{f}_s = 0$ limit, by dotted lines. We can find two solution branches for fixed $\bar{f}_s$. These branches merge at some critical radius over which a solution disappears. This is because the non-trivial structure of the non-Abelian field becomes as large as the scale of the Compton wavelength ($\sim 1/\mu$). That is, beyond this critical horizon radius, a non-trivial structure is swallowed into the horizon resulting in a Schwarzschild spacetime.

Moreover, we should mention that a cusp structure which appears at the critical radius is a symptom of the stability change in catastrophe theory [16]. The massive branch is unstable while the other branch is stable [12]. If f_s becomes small, the massive unstable branch approaches the colored black hole. Thus, it is plausible that the internal structure of the Skyrme black hole of the unstable branch shows similar behavior to the colored black hole when the mass of the Skyrme field is small. But, how about the other branch or how is this altered by the mass of the Skyrme field? These questions have not been considered previously.

We show typical structure ($\bar{r}$-$|C|^{-1}$) found inside the Skyrme black hole in Fig. 2 for solutions with $\bar{f}_s = 0.03$

and $\lambda_h = 0.7$ (solid lines) and 0.9 (dotted lines). For reference, we also show the corresponding colored black hole solutions and the exceptional Skyrme black hole solution $\lambda_h \sim 0.52$ where no oscillating behavior is seen (it corresponds to the Schwarzschild-like solution in the analysis below.). For field variables, we choose them to satisfy asymptotically flatness. In this figure, we find a steep peak (a local maximum) at some radius independently of the types of black holes. Below the radius, $|C|^{-1}$ exhibits a rapid deacrease to minus ten to several hundreds. To calculate this behavior correctly, it is necessary to use suitable variables as introduced in the Appendix of Ref. [4]. Similarly to the colored black hole, infinitely oscillating behavior appears in the Skyrme black hole case. Thus, the mass term of the Skyrme field do not help to avoid this behavior. It is the main difference in the internal structure between the ES system and the EYMH system. As for the Skyrme field, χ approaches some constant value toward the center. At first glance, it seems strange that χ stays at an almost constant value while $|C|^{-1}$ exhibits violent behavior. This is, however, also seen in the colored black hole case where its gauge potential w takes almost a constant value though its gradient $|w'|$ takes a large value in some extremely narrow interval [4]. Since χ is related to w by $\cos\chi = w$ in the $f_s \to 0$ limit, our result is consistent with the colored black hole case.

Comparing the Skyrme black hole with the colored black hole, the first peak of $|C|^{-1}$ appears at larger radius for $\lambda_h = 0.7$ while at smaller radius for $\lambda_h = 0.9$. The mass term gives quite complicated effects on the interior structure like this. To clarify them, we first show the relation between the horizon radius λ_h and r_m/r_h for colored black holes in Fig. 3. r_m is the radius where $|C|^{-1}$ takes a local maximum value. Multiplication signs, white circles and a dots mean that $|C|^{-1}$ takes a first, a second and a third branch of the peaks, respectively. At first glance, it may seem strange that the first branch is missing in the region $1.8 < \lambda_h < 2.5$. This can be understood as follows. For $\lambda_h \sim 1.7$, the peak is much milder compared with those in Fig. 2. When λ_h becomes large, the local maximum disappears by coincidence with the local mimimum. Similar disappearance occurs around $\lambda_h \sim 2.5$.

We show the Skyrme black hole case with $\bar{f}_s = 0.03$ in the framed region in Fig. 3 which corresponds to the magnification of the region $0.1 < r_m/r_h < 10^{-13}$ and $0 < \lambda_h < 1.4$ since the Skyrme black hole solution does not exist above $\lambda_h \gtrsim 1.15$ for $\bar{f}_s = 0.03$. The unstable and the stable branches of the Skyrme black holes are shown by a solid line and by a dotted line, respectively. The lines in this figure correspond to the first peak. We can see that the oscillating behavior is generic and the Skyrme black hole does not have a Cauchy horizon in general inspite of the influence by the mass term of the Skyrme field. Moreover, these properties do not depend on the stability of the black holes. This independence must be related to the fact that although the colored black hole itself is unstable against linear perturbation, interior oscillating structure is stable against non-linear perturbations [17]. In other words, this problem belongs to the structure of the ordinary differential equations around the center.

We can find the tendency that r_m for the Skyrme black hole is larger than that of the colored black hole on average, and that the amplitude of the oscillation is milder for the Skyrme black hole than that for the colored black hole. We can not say, however, definite things about these properties since there are exceptional solutions, which make the comparison complicated.

We finally mention these exceptional cases, where no oscillating behavior is seen. The candidates are the solutions corresponding to the points P, Q and R in Fig. 3. Three types of behaviors are considered assuming that variables are expressed by power series near the center [4,5], i.e., Schwarzschild-like, Reissner-Nortström (RN)-like and imaginary charged RN-like behaviors. By expanding the field variables

$$w = \sum_{n=0}^{\infty} w_n \bar{r}^n, \quad \bar{m} = \sum_{n=-1}^{\infty} \bar{m}_n \bar{r}^n , \qquad (19)$$

where $w := \cos\chi$, we can summerize these behaviors:

(i) Schwarzschild-like case ($\bar{m}_{-1} = 0$). In this case, we can express the above expansion in the following form,

$$w = -1 + b\bar{r}^2 + O(\bar{r}^4) \qquad (20)$$

$$\bar{m} = \bar{m}_0 - \frac{4}{\lambda_h^2}\bar{m}_0 b(\pi\lambda_h^2 \bar{f}_s^2 + b)\bar{r}^2$$

$$+ \frac{2b}{\lambda_h^2}(2\pi\lambda_h^2 \bar{f}_s^2 + b)\bar{r}^3 + O(\bar{r}^4). \qquad (21)$$

This is quite consistent with the previous result in Ref. [4] since it attributes to the EYM case in the $\bar{f}_s \to 0$ limit. The important thing is that b is *not* a free parameter for $\bar{f}_s \neq 0$ since we encounter a relation $\bar{f}_s b = 0$ in expanding Eq.(14). Thus, we can find that $w \equiv -1$ and $\bar{m} \equiv \bar{m}_0$. This means that there is not a Schwarzschild-like solution or that w approaches -1 faster than $\bar{r}^n$ ($n = 1, 2, 3 \cdots$) in $\bar{r}_h \to 0$. As we see below, our numerical analysis support the latter.

(ii) RN-like case. Below, $w_0 \neq \pm 1$ is assumed. This case contains three free parameters (w_0, c and $\bar{m}_0$) as

$$w = w_0 - \frac{w_0}{2V_0}\bar{r}^2 + \frac{c}{2V_0}\bar{r}^3 + O(\bar{r}^4), \qquad (22)$$

$$\bar{m} = -\frac{V_0^2}{2\lambda_h^2 \bar{r}} + \bar{m}_0 - 4\pi\bar{f}_s^2 V_0 \bar{r}$$

$$- w_0\left(\frac{c}{\lambda_h^2} + \frac{\bar{m}_0 w_0 \lambda_h^2}{V_0^2}\right)\bar{r}^2 + O(\bar{r}^3) . \qquad (23)$$

where $V_0 := w_0^2 - 1$.

(iii) Imaginary charged RN-like case. This case contains one free parameter w_0 as

$$w = w_0 \pm \lambda_h \bar{r} - \frac{w_0}{2V_0}\bar{r}^2 + O(\bar{r}^3), \qquad (24)$$

$$\bar{m} = \frac{V_0^2}{2\lambda_h^2 \bar{r}} \pm \frac{2w_0 V_0}{\lambda_h} + O(\bar{r}) . \qquad (25)$$

In order to search these exceptioanl cases, we have to integrate the basic equations toward the center for each Skyrme black hole solution varying the horizon radius. There is, however, another approach. We fix the horizon radius and search the suitable value of χ_h which satisfy the above conditions. This χ_h does not coincide with the value of the Skyrme black hole solution in general which satisfy the asymptotically flat condition. However, if it coincides, such solution is the exceptional one. This method was adopted in Refs. [4,5] and it was found that the point Q is the exceptional case (i). In Fig. 4, we exhibit a relation between the horizon radius λ_h and χ_h which satisfies the Schwarzschild-like condition (i) for $\bar{f}_s = 0.01, 0.02$ and 0.03 (dot-dashed lines). We choose χ_h to satisfy $\chi \to \pi$ at $\bar{r} \to 0$. We can find two solutions for each horizon radius if the parameter $\bar{f}_s$ is fixed. Turning back of solutions occurs at some critical radius ($\lambda_h \sim 0.16, 0.32, 0.48$ for $\bar{f}_s = 0.01, 0.02$ and 0.03, respectively.) below which a solution disappears. In the $\bar{f}_s \to 0$ limit, this turning back disappears and the solution of larger χ_h coincides with exact Schwarzschild solution (i.e., $\chi = \pi$). This is consistent with the colored black hole case examined in Ref. [4,5].

We also plot χ_h of the Skyrme black hole solutions for $\bar{f}_s = 0.03$ (i.e., χ_h satisfies asymptotically flatness.). We can find the intersections of these solutions with the Schwarzschild-like solutions. It means that there *are* exceptional solutions corresponding to the points P and R ($\lambda_h \sim 0.52,\ \ 1.13$).

IV. CONCLUSION

We examined internal structure of the Skyrme black hole and compared it with the colored black hole case. Although the gravitational structures and the thermodynamical properties of the Skyrme black hole are similar to those of the sphaleron black hole in the EYMH system, internal structure is quite different qualitatively from the sphaleron black hole because of the absence of the scalar field. Similarly to the colored black hole, the mass function of the Skyrme black hole exhibits oscillating behavior. The amplitude of the oscillations of the metric function tends to become smaller than that of the colored black hole due to the mass of the Skyrme field. It is difficult, however, to conclude that it is a generic feature because of the existence of the exceptional solutions where oscillating behavior does not happen. We also find exceptional Schwarzschild-like solutions which exist both for stable and unstable branches.

[1] R. Bartnik and J. McKinnon, Phys. Rev. Lett. **61**, 141 (1988).

[2] As a review paper see K. Maeda, Journal of the Korean Phys. Soc. **28**, S468, (1995), and M. S. Volkov and D. V. Gal'tsov, Phys. Rep. **319** 1 (1999).

[3] P. Bizon, Acta. Phys. Pol. B **25**, 877 (1994).

[4] E. E. Donets, D. V. Gal'tsov, and M. Yu. Zotov, Phys. Rev. D **56**, 3459 (1997); D. V. Gal'tsov, E. E. Donets, and M. Yu. Zotov, gr-qc/9712003; ibid., gr-qc/9712024; ibid., hep-th/9709181; ibid., JETP Lett. **65**, 895 (1997).

[5] P. Breitenlohner, G. Lavrelashvili, and D. Maison, Nucl. Phys. B **524**, 427 (1998); ibid., gr-qc/9708036; ibid., gr-qc/9711024.

[6] D. V. Gal'tsov, E. E. Donets, gr-qc/9706067.

[7] O. Sarbach, N. Straumann, and M. S. Volkov, gr-qc/9709081.

[8] H. Luckock and I. G. Moss, Phys. Lett. B **176**, 341 (1986); H. Luckock, in *String theory, quantum cosmology and quantum gravity, integrable and conformal invariant theories*, eds. H. de Vega and N. Sanchez, (World Scientific, Singapore, 1986), p. 455.

[9] S. Droz, M. Heusler and N. Straumann, Phys. Lett. B **268**, 371 (1991).

[10] P. Bizon and T. Chmaj, Phys. Lett. B **297**, 55 (1992).

[11] D. V. Gal'tsov, private communication.

[12] K. Maeda, T. Tachizawa, T. Torii and T. Maki, Phys. Rev. Lett. **72**, 450 (1994); T. Torii, K. Maeda and T. Tachizawa, Phys. Rev. D **51**, 1510 (1995); T. Tachizawa, K. Maeda and T. Torii, Phys. Rev. D **51**, 4054 (1995).

[13] T.Tamaki, K. Maeda and T. Torii, Phys. Rev. D **57**, 4870 (1998); *ibid.*, **60**, 104049 (1999).

[14] T. H. R. Skyrme, Proc. R. Soc. London **260**, 127 (1961); J. Math. Phys. **12**, 1735 (1971).

[15] For a particle-like solution (Skyrmion), the value of χ at the origin must be πn, where n is an integer and $|n|$ denotes the winding number of the Skyrmion. In the case of the black hole solution, it is topologically trivial. But W_n defined by (18) is close to n, so we shall also call it the "winding" number.

[16] T. Poston and I. Stewart, *Catastrophe Theory and Its Applications*, Pitman, London (1978); R. Thom, *Strucure Stability and Morphogenesis*, Benjamin (1975).

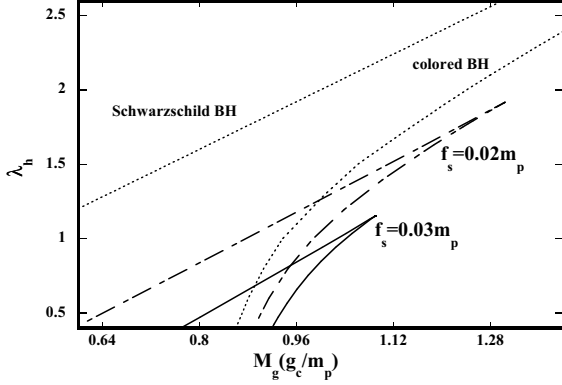[17] E. E. Donets, M. N. Tentyukov, and M. M. Tsulaia, Phys. Rev. D **59**, 064008 (1999).

FIG. 1. M-λ_h diagram of Skyrme black holes with $\bar{f}_s = 0.02$ and 0.03. We also show the results of the colored and Schwarzschild black holes for reference.
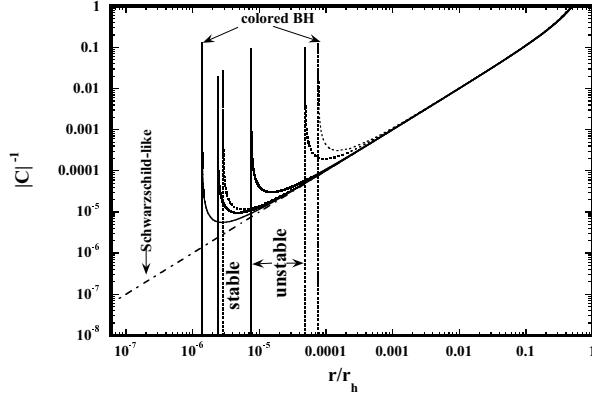

FIG. 3. λ_h-r_m/r_h diagram of the colored black holes. A multiplication sign, a white circle and a black circle mean that $|C|^{-1}$ takes a first, a second and a third peak, respectively. We also show the unstable and the stable branches of the Skyrme black hole in the framed region ($0.1 < r_m/r_h < 10^{-13}$ and $0 < \lambda_h < 1.4$) which are shown by a solid line and by a dotted line, respectively.

FIG. 2. $\bar{r}$-$|C|^{-1}$ diagram of Skyrme black holes with $\bar{f}_s = 0.03$ and colored black holes. We consider both unstable and stable branches with the horizon radii $\lambda_h = 0.7$ (solid lines) and $\lambda_h = 0.9$ (dashed lines). We also show the corresponding colored black holes and the exceptional Skyrme black hole solution $\lambda_h \sim 0.52$ where there is no oscillating behavior.
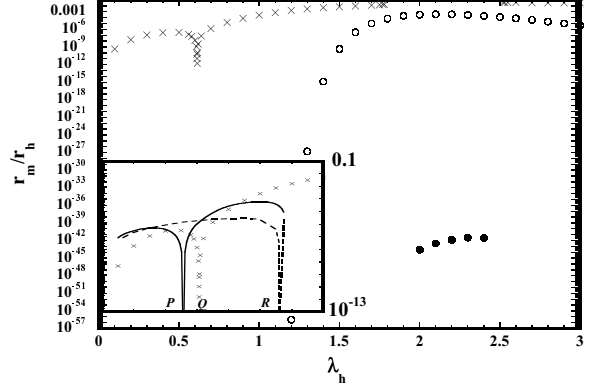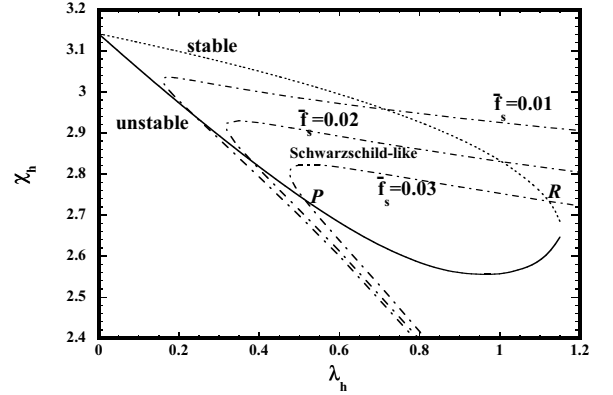

FIG. 4. λ_h-χ_h diagram of the Skyrme black holes. χ_h to satisfy the asymptotically flatness for $\bar{f}_s = 0.03$ is shown by a dotted line (the stable branch) and by a solid line (the unstable branch) and χ_h to satisfy the Schwarzschild-like condition for $\bar{f}_s = 0.01$, 0.02 and 0.03 are shown by dot-dashed lines.